Tanzania Journal of Science 46(2): 205-215, 2020
ISSN 0856-1761, e-ISSN 2507-7961
© College of Natural and Applied Sciences, University of Dar es Salaam, 2020

Structural, Mineralogical and Quantitative Characterizations of Compositions of Products Linked to Explosive Volcanic Eruption at Haleakala, USA

Aderemi B Alabi[1], Ibukun S Akinsola[1,2*], Saminu Olatunji[3], Comfort Ogunyinka[1] and Oluwatoyin Osanyinlusi[1]

[1] *Department of Physics, University of Ilorin, Ilorin, Nigeria.*

[2]*Department of Physical and Mathematical Sciences (Physics Unit), Crown-Hill University, Eiyenkorin, Ilorin, Nigeria.*

[3]*Department of Geophysics, University of Ilorin, Ilorin, Nigeria.*

[*]*Corresponding author, e-mail: siakinsola711@gmail.com*

Co-authors e-mail addresses: remi050970@gmail.com (Alabi), sam61ng@gmail.com (Olatunji), ogunyinkacomfort7@gmail.com (Ogunyinka), adetolusi@gmail.com (Osanyinlusi)

Received 24 December 2019, Revised 14 April 2020, Accepted 17 April 2020, Published June 2020

DOI: https://dx.doi.org/10.4314/tjs.v46i2.2

Abstract

This research focused the analysis vis-à-vis structural, mineralogical and quantitative characterizations of the samples which appeared to be formed from leftover of volcanic eruption sourced from basaltic magma obtained from Haleakala Hill, USA. The results show the presence of natural minerals like pyrolusite, zincite, magnetite, quartz, and diopside with their compositional concentrations in the samples. The geophysical analysis done corroborates the results obtained from the Scanning Electron Micrograph, which confirms the porosity of one of the samples. The X-Ray Diffraction results reveal the average grain sizes of the samples to range between 16 nm and 25 nm. Sample 'A' showed 4.693% weight increase, while sample 'B' showed 7.724% when soaked for some days. This research project prospects in harnessing natural minerals from products of volcanic eruption, though an occurrence regarded as a natural disaster. The work suggests an alternative route to mining of minerals, by exploring the contents of the products of this so-called disaster.

Keywords: Volcanoes; Minerals; Magma; Characterization; Mining; Explosion

Introduction

A good number of land resources are formed by volcanoes. In oceans, there are numerous sporadic islands; big and small. The Hawaiian Islands which are located in the Pacific Ocean are good examples constructed by volcanoes. Continuous oceanic volcano eruptions and magma pouring into the ocean constructing islands make the young Hawaiian Islands keep growing. This experience is also seen in Iceland and Reunion (Liu et al. 2012).

In explosive eruptions, magma is fragmented by rapid exsolution of dissolved volatile components to produce pyroclastic materials. Fine-grained portions of these materials are called volcanic ashes, and are distributed over a wide area far from the source volcano according to the dominant wind direction above the volcano. Magma is usually composed of silicate melt and crystallized materials (known as phenocryst). Hence, volcanic ash consists of minerals and volcanic glass. Onuiri et al. (2015) describes mineral resources as non-

living naturally occurring matters which consist of solid inorganic materials or petrified organic matter including industrial mineral, valuable metals, which can both be discovered in and on the earth's crust in a pattern, quantity, of such a grade and quality with realistic expectations for cost effective extraction.

The link that exists genetically between magmas and formation of ore deposit has been by studies of fossil hydrothermal systems connected with magmatic intrusions at depth. Nevertheless, the functions of processes that involve explosive volcanic as active agents of mineralization are not explored due to the fact that metals and volatiles are always released into the atmosphere during the eruption of these arc volcanoes (Ovalle et al. 2018).

Researchers in the area of materials science and geology might have not being awakened to the fact that "something to eat can come from the eater", that is, a natural disaster can give products which have contents to explore for the growth of science, technology and hence economy of nations at this advantage. The motivations for this study are the fact that alternative to mining of some natural minerals for industrial applications is not yet well explored by geologists and geophysicists and also to examine the economic importance of the so-called 'natural disaster' – volcanic eruptions, by climate changes.

In this work, we investigated, using suitable characterizations techniques, the minerals present and their compositional concentrations in the samples obtained from the Haleakala hill, Hawaii, United States of America and discuss the prospects they hold if harnessed for industrial and educational purposes, as alternative to mining for similar minerals from other land structures.

Materials and Methods

The samples labelled 'A' and 'B' obtained in September, 2018 on the Haleakala hill, USA, which is on the coordinates $20°\,47'\,18''N$ and $156°34'\,1''W$ and elevation 9760 ft above the sea level (see the geographical map in Figure 1) were crushed into particulate forms using an electric industrial grinder. Sample 'A' was picked on the top of the hill, while sample 'B' was from a few meters downward from the top of the hill. The sample A appeared younger geologically (light in appearance) than sample 'B' (darker than sample 'A' in appearance).

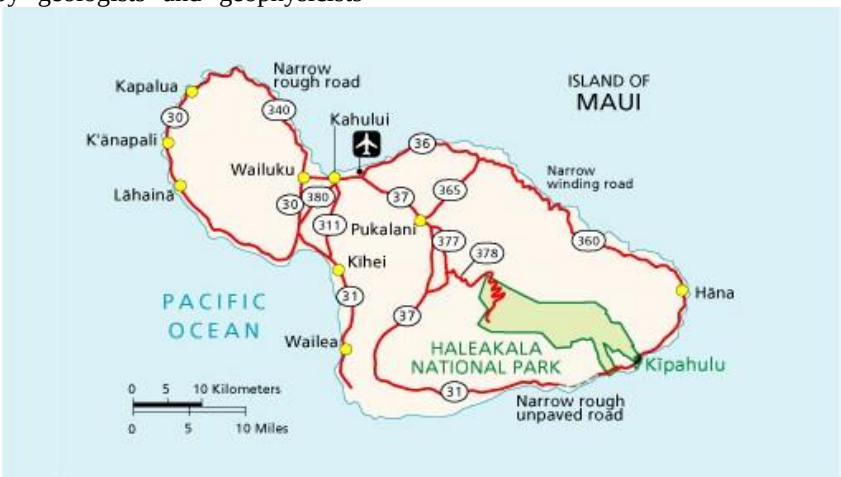

Figure 1: Map showing the location of the volcanic island referred to in the article.

The numbers on the map could be describing something else; however, the interest in this work is to picture the location of the samples in consideration.

The samples, after being crushed, were split to form a loose powder. Pulverizing was done. This plays a vital role in reducing the effects of particles size and it works by making all the particles in the specimen of a consistent size. The loose powder was then placed in the pelletizer to form pellet. The pelletizer produces pellets which are flat and smooth samples to be characterized. The pellet should be around 3 mm thick. If the sample is thinner than this, it could be considered using more sample and the opposite is true if the sample is much thicker than 3 mm. Importantly, consistency in size is the key. Hence, the sample needs to be weighed before pressing. The examples of pictures of pellets are shown in Figure 2.

Figure 2: Examples of images of pellets.

The pelletized samples were characterized to obtain the structural, mineralogical, and elemental compositions of the materials using the Scanning Electron Microscopy (SEM), X-Ray Diffraction (XRD), and Energy Dispersive X-Ray Fluoresence (ED-XRF), respectively. The SEM is done so as to get the images of the structures of the sample particles which will entail the morphological descriptions of the samples. The small pellets formed were ensured to be dry and placed in the sample holder of the scanning electron microscope used for obtaining the micrograph. The scanning electron microscope used was ZEISS made. The EHT used for the microscope was 10.00 kV and width sizes were 11.0 mm and 11.5 mm.

The XRD is a technique used for determining the atomic and molecular structures of a crystalline material, in which the crystalline structure causes a beam of incident X-rays to diffract into many specific directions. The X-Ray Diffractometer used was EMPYREAN, with radiation of wavelength 1.540598 Angstrom as k-Alpha1 and 1.544426 Angstrom as k-Alpha2. The anode material was copper, Cu. The scan range was 4.989299997 at scan step size of 0.0262606 and the scan type was continuous. The time per step was 29.07 seconds. The measurement temperature was 25 °C. The generator settings were 40 mA and 45 kV. The powder XRD used extensively helps to identify the phases by measuring the diffraction angles and intensities of the diffracted beams, and comparing the resulting diffraction patterns to a reference database of diffraction data that gives the mineralogical contents of the samples. The intensity of the diffracted X-rays is measured as a function of the diffraction angle 2θ and the specimen's orientation (Brundle et al. 1992). The porosity of the sample was tested with the uncrushed (whole) sample being soaked inside a container of water. This is to determine to what extent it can hold water. For the ED-XRF, the live time during the characterization technique was 1000 seconds and the tube current was 0.050 mA. The method applied was direct comparison of count rates.

Results and Discussion

Geological and geophysical analyses

The images of the samples linked to the products of volcanic eruption as obtained from the location are shown in Figure 3 (a) and (b).

A B

Figure 3: Rock samples (A & B).

Geological analysis

The two samples, being from Haleakala National Park, USA on the coordinate $20^{\circ}\,47'\,18''N$ and $156^{\circ}\,34'\,1''W$ and elevation 9760 ft above the sea level,

appeared to be leftover of volcanic eruption sourced from basaltic magma. The samples are dark-grey to dark (melanocratic) with fine-textured (aphanitic). They comprised of < 1 mm to 3 mm sized particles welded into porous and poorly-porous rock masses. This evident high probability of forming from volcanic eruption(s) whereby ejected hot magmas broke up in air into globules that cooled and crystallised into millimicrons-sized particles (or volcanic dust). The dust particles were hot and would collide with each other to fuse into successively bigger, micro-sized (volcanic ash) and millimeter-sized (lump) particles. The welding of these fine particles produced rock masse(es) with a variable inter-particle (or pore) spaces and cubical densities.

Geophysical analysis (density and porosity tests)

Based on Parasnis (1962)'s recommendations, the *in situ* cubical density of rocks lies between the dry and wet densities. Hence, using Archimedes' principle, the dry and wet densities of sample 'A' are 2.402 g cm^{-3} and 2.355 g cm^{-3} with average density of 2.379 g cm^{-3}, while for 'B' are 2.609 g cm^{-3} and 2.325 g cm^{-3}, with average density of 2.467 g cm^{-3}. The common density is 2.423 g cm^{-3}. Sample 'A' showed 4.693% weight increase, while sample 'B' showed 7.724% when soaked for some days. By deductions, sample 'B' is of high porosity and low consolidation than sample 'A'. This could just be as a result of volcanisms of different times. Thus, sample 'A' could be geologically younger than sample 'B'. Also, average density obtained is in the range of that of the upper continental crustal density which is 2.67 g cm^{-3} above sea level (as suggested by Osazuwa et al. 1981). This suggested that the volcanic magmas that formed the samples originated from the upper crust above the sea level in the earth's interior.

Structural and Mineralogical Compositions

(a) X-ray diffraction analysis

The X-ray diffraction technique employed revealed the structural and mineralogical contents of the samples. For sample A, the peaks considered, among others (Figure 4), at 2θ angle 20.5°, 27.9° are for the mineral *diopside*. The 2θ angle 29.9° and 35.5° for *magnetite* correspond to diffraction from planes (2 2 0) and (3 1 1), respectively, which are very close to the expected values of about 30.1° and 35.8° in the database from JCPDS card No [19-0629] for magnetite (Hossain et al. 2017). The other mineral in the sample is *quartz*. Diopside is a brittle monoclinic mineral with chemical formula $MgCaSi_2O_6$. It is a precursor of chrysolite by hydrothermal alterations and magmatic differentiation. Quartz has a formula SiO_2–silica or silicon dioxide. It finds applications in glass making, abrasive, foundry sand, etc. Magnetite is with chemical formula $Fe^{2+}Fe_2^{3+}O_4$. It is black, grey with brownish tint in reflected sun. The sample characterized portrays these features.

The grain sizes for the two samples were estimated using the *Debye-Scherrer's* equation: $g = \frac{k\lambda}{\beta Cos\theta}$ (1)

λ, β, and θ represent the wavelength of the X-ray source, the full width at half maximum (FWHM), and the Bragg angle, respectively (Akinsola et al. 2017).

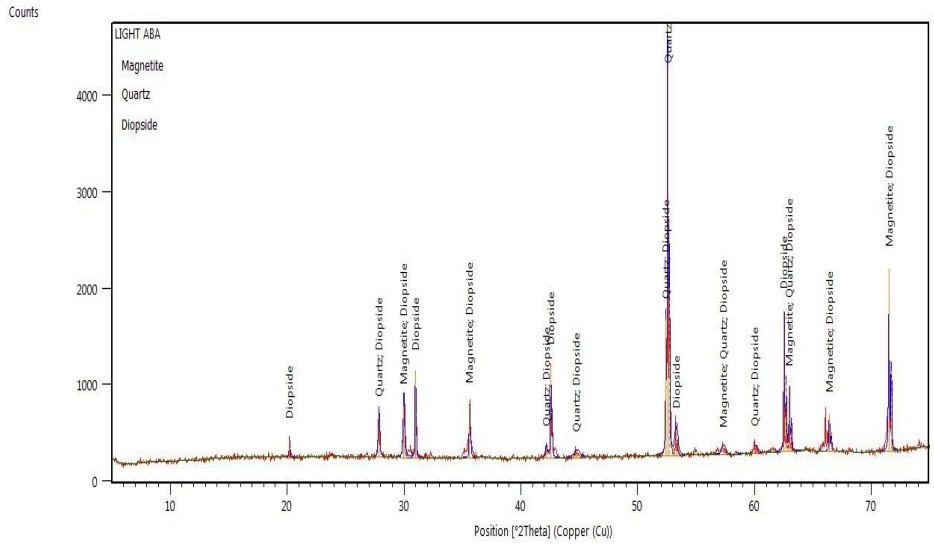

Figure 4: XRD pattern for the sample A (light).

Table 1: Values of grain sizes of the compositions of sample A

2θ (Degree) of distinct diffraction peaks in Sample A	Grain sizes, g (nm)	Constituent present
20.5	33.8	Diopside
27.9	21.4	Quartz, Diopside
35.5	17.4	Magnetite, Diopside

Table 2: Values of grain sizes of the compositions of sample B

2θ (Degree) of distinct diffraction peaks in Sample B	Grain size, g (nm)	Constituent present
27.5	17.1	Pyrolusite-MnO_2
35.5	8.7	Zincite- ZnO
57.5	23.6	MnO_2 & ZnO

In the XRD pattern for sample B (Figure 5), the peaks considered, among others, at 2Θ angle 27.5°, 35.5° and 57.5° correspond to diffraction from planes (3 1 0), (1 0 1) and (1 1 0), respectively, which are very close to the expected values from JCPDS No. [44 - 0141] for pyrolusite and [36 -1451] for zincite (ZnO). Sample B contains minerals; pyrolusite which is a source of manganese and mincite, a source of zinc. Pyrolusite, being tetragonal and zincite, hexagonal is confirmed from the JCPDS card used for comparing the obtained X-ray diffraction patterns of the samples with what are in the database for the two major minerals in the samples. Figure 6 represents the crystal structure of zincite.

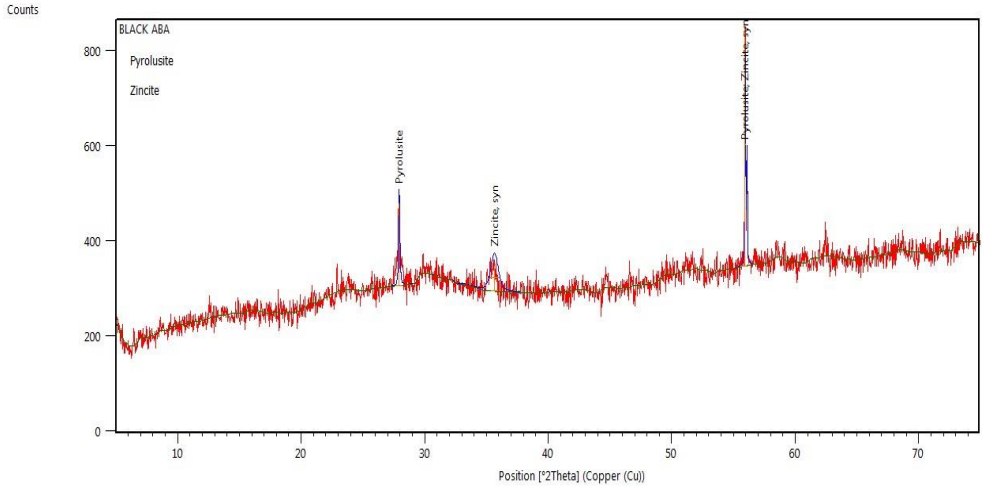

Figure 5: XRD pattern for the sample B (dark).

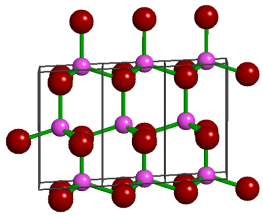

Figure 6: Crystal structure of zincite (obtained from mineral structure data, University of Colorado 2020; http://ruby.colorado.edu/~smyth/min/zincite.html).

Also, the polyhedral structure of the pyrolusite crystal is presented in Figure 7. The figure could also stand for rutile titanium(IV) oxide. According to Post (1999), there exist three known mineral poly-morphs of MnO_2; only pyrolusite is the most stable and abundant among them. The others are ramsdellite and nsutite. In the pyrolusite (β-MnO_2), single chains of edge-sharing $Mn(IV)O_6$ octahedral sharecorners with neighbouring chains to form a framework structure containing tunnels with square cross sections that are one octahedron by one octahedron (1 x 1) on a side. The structure is analogous to that of rutile (TiO_2).

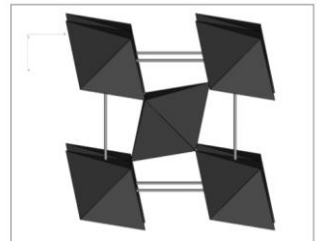

Figure 7: Polyhedral structure of pyrolusite crystal structure (Post 1999).

This can be leached using a suitable leaching method to obtain the needed element, e.g. manganese. This can substitute the costs and efforts employ in mining for manganese. Similar step could be used for obtaining zinc from zincite in lieu of mining processes. The products of volcanic eruption, if positively harnessed, could result in the eventual production of metals, other elements and/or minerals which could be for industrial application(s).

The country, USA where the location of the volcanic eruption is situated could explore the extraction of these natural minerals from the products of volcanic eruption for educational, scientific and industrial purposes, as an alternative to geological mining processes for the same minerals.

The average grain sizes obtained for the two samples A and B, based on the expected

dominant resources in each, are 24.18 nm and 16.47 nm, respectively. From the XRD patterns of the samples, it could be said that the materials are highly crystalline in nature, especially sample A. The smaller particle size of sample B than A could owe to the high porosity of the sample compared to the latter. The relatively small grain sizes in nano scale projects confirm that the natural semiconductor material is indeed a nanomaterial, as seen in the constituents – MnO_2, ZnO, Fe_2O_4, which is discussed in the XRD analysis section.

(b) Scanning electron micrograph of the samples

The morphology; shape, form and size of a material is examined by the scanning electron microscopy (SEM). The scanning electron micrographs of the samples are presented in Figures 8 (a) and (b). The SEM image of sample A as given by Figure 8 (a) reveals the particles in the sample to be homogenous and compact, though porous a little. The micrograph of sample B as in Figure 8 (b) shows the composition to be of a porous and homogenous morphology, though non-uniform. The porosity as revealed by the microghraph confirms the results discussed in session of geophysical analysis, although sample B is highly porous than sample A. This partly agrees with the findings of Gorbach et al (2018), who reported that at a micrograph magnification of 400 µm the products of volcanic eruption characterized showed porous and dense fragments of the minerals.

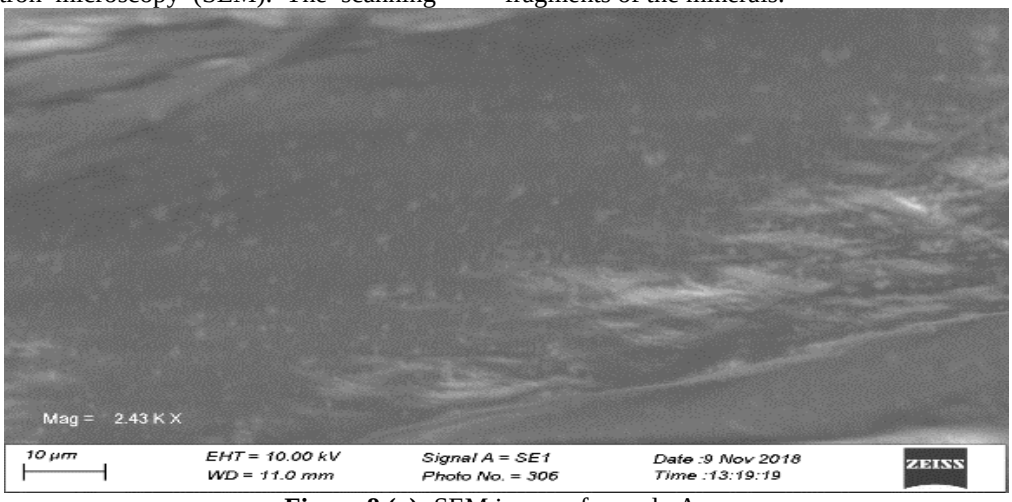

Figure 8 (a): SEM image of sample A.

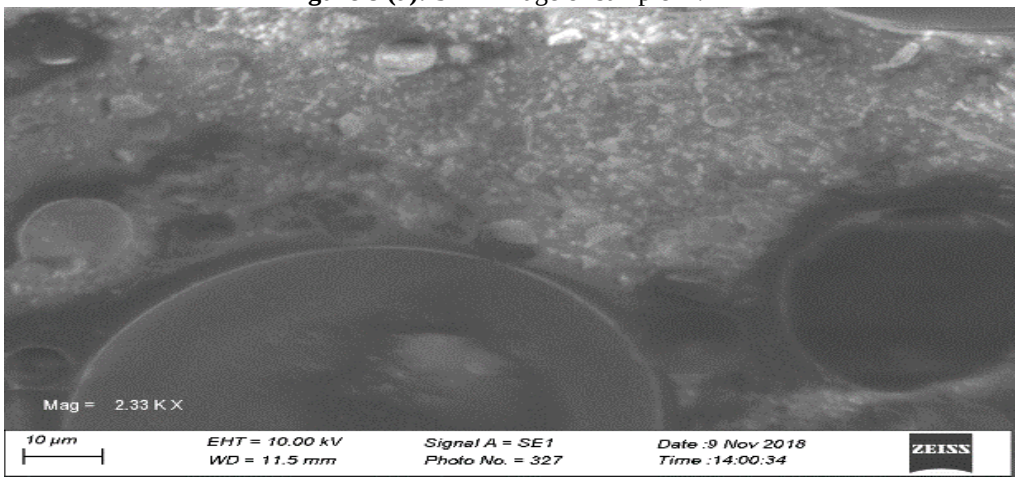

Figure 8 (b): SEM image of sample B.

Quantitative analysis

According to Olsen and Fruchter (1986), there is an imperative need to have the elemental composition of volcanic ash by the volcanologist or geologist in order to determine what occurs during a volcanic eruption. Elemental composition is essential to ascertain the mineralogical classification of the ash (i.e., basalt, andesite, dacite, and rhyolite, etc).

Energy Dispersive X-Ray Fluoresence (ED-XRF) reveals the elemental compositions and the concentrations thereof in each sample.

Figures 9 and 10 show the spectra of the ED-XRF analyses carried out on the two samples, while Tables 3 and 4 give the concentrations in %W and parts per million (ppm) of the elemental compositions of the samples A and B, respectively after being interpreted with a suitable computer software.

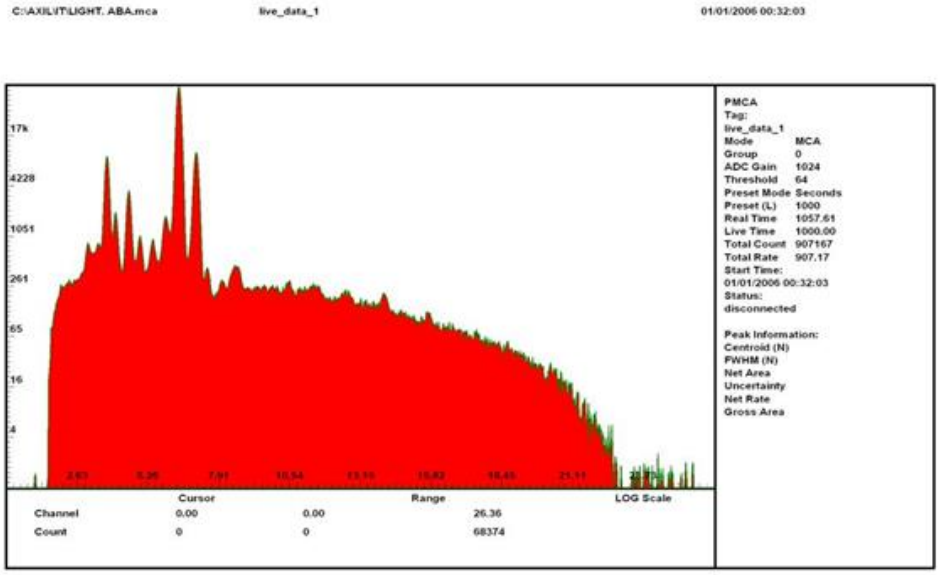

Figure 9: ED-XRF spectra for sample A.

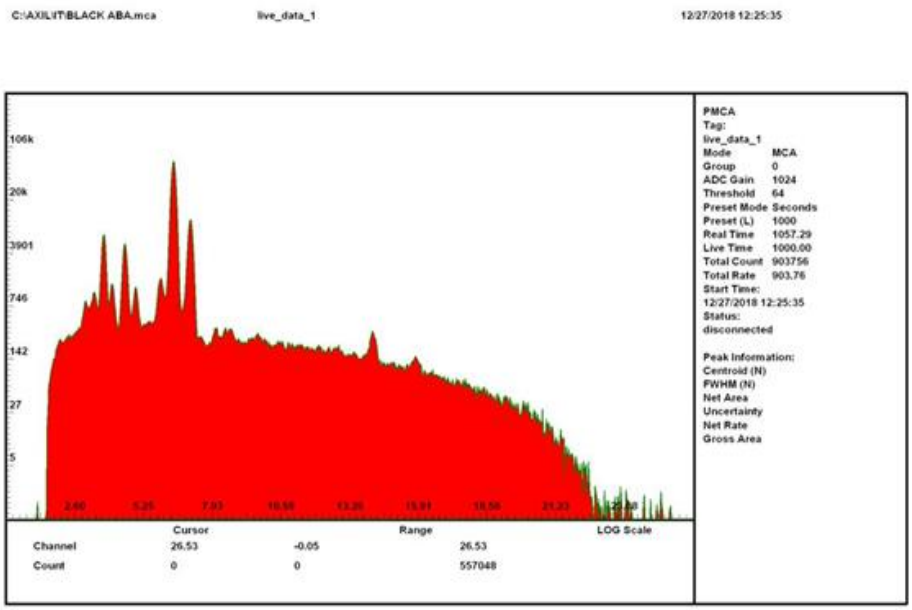

Figure 10: ED-XRF spectra for sample B.

From the mineralogical contents of sample A as revealed by the XRD results, the minerals present are diopside, quartz and magnetite, aside from several other metal elements present as impurities with their small, non-distinct peaks in the XRD patterns. Considering the chemical formula of diopside, $MgCaSi_2O_6$, and the concentration of calcium (Ca) which could be that of the part of diopside in the sample is given as about 5.8 %w. The other mineral found in the sample, magnetite has iron (Fe) as a major metal elemental constituent and the concentration of Fe given as of about 8.5 %w confirms how rich the sample is in magnetite, which is a prospective source of iron. These products of volcanic eruption can be harvested in large quantities for the extraction of these minerals and/or leached for needed metal elements composed of.

Sample B was composed of pyrolusite (MnO_2), zincite (ZnO) minerals with distinct peaks as revealed by the XRD patterns and several other metal elements like potassium, calcium, iron, to mention a few as seen in Figure 5. Apart from the distinct minerals revealed by the distinct peaks in the XRD patterns of the sample B, the several other elements shown by the XRF results could be regarded as impurities, since the material is earthy. The interest in this work are the mineralogical compositions, which could substitute mining for similar minerals. Pyrolusite has manganese (Mn) as the major metal element. Table 3 reveals the concentrations of each element found in the sample as obtained from the ED-XRF analyses carried out. Manganese had a concentration of about 2419.665 ± 149.472 ppm. This is higher than the concentration of zinc (Zn) which is within the range of 155 ppm to 212 ppm. This could be attesting to the fact that pyrolusite is the major mineral constituent of sample B, while zincite is just an inclusion. Manganese can be richly explored in the product of a volcanic eruption occurrence in this region of the USA where the samples were obtained.

Table 3: Elemental composition and concentrations of sample A

Elements present	**Concentration**	
	Range (min – max)	**Mean ± SD (n = 2)**
Potassium, K	2437.136 – 3389.23	2913.183 ± 476.047 ppm
Calcium, Ca	5.669 – 6.021	5.845 ± 0.176 %w
Manganese, Mn	2270.193 – 2569.137	2419.665 ± 149.472 ppm
Iron, Fe	8.446 – 8.628	8.537 ± 0.091 %w
Nickel, Ni	188.666 – 206.144	197.405 ± 8.739 ppm
Copper, Cu	66.76 – 77.622	72.191 ± 5.431 ppm
Zinc, Zn	155.601 – 212.121	183.861 ± 28.260 ppm
Gallium, Ga	< 4.511	< 4.511 ppm
Lead, Pb	21.412 – 25.53	23.471 ± 2.059 ppm
Selenium, Se	42.191 – 48.019	45.105 ± 2.914 ppm
Bromine, Br	6.803 – 13.003	9.903 ± 3.100 ppm
Rubidium, Rb	16.21 – 24.518	20.364 ± 4.154 ppm
Strontium, Sr	208.762 – 218.192	213.477 ± 4.715 ppm
Yttrium, Y	< 18.699	< 18.699 ppm
Zirconium, Zr	73.007 – 93.137	83.072 ± 10.065 ppm
Niobium, Nb	51.546 – 82.474	67.010 ± 15.464 ppm
Molybdenum, Mo	< 86.736	< 86.736 ppm

Table 4: Elemental composition and concentration of sample B

Elements present	**Concentration**	
	Range (min - max)	**Mean ± SD (n = 2)**
Potassium, K	4726.471 – 5395.715	5061.093 ± 334.622 ppm
Calcium, Ca	3.851 – 4.013	3.932 ± 0.081 %w
Titanium, Ti	1.657 – 1.765	1.711 ± 0.054 %w
Vanadium, V	946.224 – 1185.684	1065.954 ± 119.730 ppm
Chromium, Cr	327.464 – 485.678	406.571 ± 79.107 ppm
Manganese, Mn	2590.443 – 2985.599	2788.021 ± 197.578 ppm
Iron, Fe	8.58 – 8.76	8.670 ± 0.090 %w
Nickel, Ni	57.946 – 70.054	64.000 ± 6.054 ppm
Copper, Cu	104.164 – 121.303	112.734 ± 8.569 ppm
Zinc, Zn	97.236 – 122.62	109.928 ± 12.692 ppm
Gallium, Ga	< 15.953	< 15.953 ppm
Lead, Pb	< 14.628	< 14.628 ppm
Selenium, Se	< 17.975	< 17.975 ppm
Bromine, Br	< 21.461	< 21.461 ppm
Rubidium, Rb	< 28.364	< 28.364 ppm
Strontium, Sr	521.209 – 575.302	548.302 ± 27.093 ppm
Yttrium, Y	< 65.039	< 65.039 ppm
Zirconium, Zr	153.578 – 221.784	187.784 ± 34.206 ppm
Niobium, Nb	< 150.773	< 150.773 ppm

Conclusion

The structural, mineralogical and quantitative characterizations of the samples which appeared to be formed from leftovers of volcanic eruption sourced from basaltic magma obtained from Haleakala Hill, USA were carried out in this work. The presence of natural minerals and their compositional concentrations in the samples were confirmed from the characterizations carried out. This research gives informative prospects in harnessing natural minerals in products of volcanic eruption, though an occurrence regarded as a natural disaster. The work suggests an alternative route to mining of minerals, by exploring the contents of the products of this so-called disaster- volcanic eruption.

Acknowledgement

The authors express sincere appreciations to the management of Haleakala National Park, Hawaii, USA for the samples obtained there. Also, the Centre for Energy Research and Development, Obafemi Awolowo University, Ile-Ife, Nigeria is appreciated for one of the characterizations carried out there.

Declaration of Interest

The authors declare that there is no conflict of interest whatsoever on this research work.

References

Akinsola SI, Obere CJ, Oyelade OV, Adedokun G, Alabi AB 2017 Chemical composition of solid minerals from Lokoja and Jos in North Central Nigeria. *FULafia J. Sci. Technol.* 3(2): 58-62.

Brundle CR, Evans Jr. CA, Wilson S 1992 Encyclopedia of materials characterization: Surfaces, Interfaces, Thin Films; Materials characterization series, Butterworth-Heinemann, Reed Publishing, USA, pp.16.

Gorbach NV, Plechova AA, Manevich TM, Portnyagin MV, Philosofova TM, Samoilenko, SB 2018 The composition of volcanic ash and the dynamics of the 2013-2016 Zhupanovsky volcanic eruption. *J. Volcanol. Seismol.* 12(3):155-171.

Hossain MK, Pervez FM, Mia MNH, Mortuza AA, Rahaman MS, Karim MR, Islam JMM, Ahmed F, Khan MA 2017 Effect of dye extracting and sensitization time on photovoltaic performance of natural dye sensitized solar cells. *Results in Physics* 7: 1516-1523.

Liu J, Liu J, Chen X and Guo W 2012 Volcanic natural resources and volcanic landscape protection: An overview. In *Updates in Volcanology-New Advances in Understanding Volcanic Systems*. IntechOpen.

Olsen KB and Fruchter JS 1986 Identification of the physical and chemical characteristics of volcanic hazards. *Am. J. Publ. Health (AJPH)* Chapter 5. 76: 45-52.

Onuiri EE, Ogbonna AE, Alli-Shehu B and Maduakolam C 2015 Mineral resources management information system. *Eur. J. Comput. Sci. Inform. Syst.* 3(2): 13-23.

Osazuwa IB, Ajakaiye DE, and Verheijen PJT 1981 Analysis of the structure of part of the upper Benue rift valley on the basis of new geophysical data. *Earth Evolut. Sci.* 2: 126-135.

Ovalle JT, La Cruz NL, Reich M, Barra F, Simon AC, Konecke BA, Rodriguez-Mustafa MA, Deditius AP, Childress TM and Morata D 2018 Formation of massive iron deposits linked to explosive volcanic eruptions. *Sci. Rep.* 8(1): 1-11.

Parasnis DS 1962 *Principle of Applied Geophysics*. Chapman and Hall limited, London, pp. 176.

Post JE 1999 Manganese oxide minerals: Crystal structures and economic and environmental significance. *Proc. Natl Acad. Sci.* USA 96(7): 3447-3454.

University of Colorado 2020 Mineral Structure data- Zincite group. http://ruby.colorado.edu/~smyth/min/zincite.html (assessed on 14th April, 2020).